Journal Pre-proof

Dissolved major and trace geochemical dynamics in Antarctic lacustrine systems

Karina L. Lecomte, Paula A. Vignoni, Cecilia V. Echegoyen, Pia Santolaya, Kateřina Kopalová, Tyler J. Kohler, Matěj Roman, Silvia H. Coria, Juan M. Lirio

PII: S0045-6535(19)32177-0

DOI: https://doi.org/10.1016/j.chemosphere.2019.124938

Reference: CHEM 124938

To appear in: *ECSN*

Received Date: 31 May 2019

Revised Date: 9 August 2019

Accepted Date: 21 September 2019

Please cite this article as: Lecomte, K.L., Vignoni, P.A., Echegoyen, C.V., Santolaya, P., Kopalová, Kateř., Kohler, T.J., Roman, Matě., Coria, S.H., Lirio, J.M., Dissolved major and trace geochemical dynamics in Antarctic lacustrine systems, *Chemosphere* (2019), doi: https://doi.org/10.1016/j.chemosphere.2019.124938.

DISSOLVED MAJOR AND TRACE GEOCHEMICAL DYNAMICS IN ANTARCTIC LACUSTRINE SYSTEMS

Karina L. Lecomte[1,2*], Paula A. Vignoni[2,3,4], Cecilia V. Echegoyen[1], Pia Santolaya[2], Kateřina Kopalová[5], Tyler J. Kohler[5,6], Matěj Roman[7], Silvia H. Coria[8], Juan M. Lirio[8]

[1] *Centro de Investigaciones en Ciencias de la Tierra (CICTERRA), CONICET/Universidad Nacional de Córdoba, Av. Vélez Sarsfield 1611, X5016CGA Córdoba, Argentina.* karina.lecomte@unc.edu.ar, cvechegoyen@hotmail.com

[2] *Facultad de Ciencias Exactas Físicas y Naturales, Universidad Nacional de Córdoba, Av. Vélez Sarsfield 1611, X5016CGA Córdoba, Argentina.* vignoni.paula@gmail.com, mpiasantolaya@gmail.com

[3] *Institute of Geosciences, Potsdam University, Karl-Liebknecht-Straße. 24-25, 14476 Potsdam-Golm, Germany.* pauvignoni@uni-potsdam.de

[4] *Climate dynamics and landscape evolution, German Research Centre for Geoscience GFZ, Telegrafenberg, 14473 Potsdam, Germany.* pvignoni@gfz-potsdam.de

[5] *Department of Ecology, Faculty of Science, Charles University, Viničná 7, 128 44, Praha 2, Czechia.* katerina.kopalova@natur.cuni.cz,

[6] *Current address: Stream Biofilm and Ecosystem Research Laboratory, School of Architecture, Civil and Environmental Engineering, École Polytechnique Fédérale de Lausanne, CH-1015 Lausanne, Switzerland.* tyler.j.kohler@gmail.com

[7] *Department of Geography, Faculty of Science, Masaryk University, Kotlářská 2, 611 37, Brno, Czechia.* matej.roman@gmail.com

[8] *Instituto Antártico Argentino, 25 de Mayo 1143, San Martín, Prov. Buenos Aires, Argentina.* silviahcoria@gmail.com, liriojm@gmail.com

**Corresponding author (email address: karina.lecomte@unc.edu.ar)*

ABSTRACT

Clearwater Mesa (James Ross Island, northeast Antarctic Peninsula) provides a unique opportunity to study solute dynamics and geochemical weathering in the pristine lacustrine systems of a high latitude environment. In order to determine major controls on the solute composition of these habitats, a geochemical survey was conducted on 35 lakes. Differences between lakes were observed based on measured physico-chemical parameters, revealing neutral to alkaline waters with total dissolved solids (TDS) <2500 mg L^{-1}. Katerina and Trinidad-Tatana systems showed an increase in their respective TDS, total organic carbon values, and finner sediments from external to internal lakes, indicating an accumulation of solutes due to weathering. Norma and Florencia systems exhibited the most diluted and circumneutral waters,

likely from the influence of glacier and snow melt. Finally, isolated lakes presented large variability in TDS values, indicating weathering and meltwater contributions at different proportions. Trace metal abundances revealed a volcanic mineral weathering source, except for Pb and Zn, which could potentially indicate atmospheric inputs. Geochemical modelling was also conducted on a subset of connected lakes to gain greater insight into processes determining solute composition, resulting in the weathering of salts, carbonates and silicates with the corresponding generation of clays. We found CO_2 consumption accounted for 20-30% of the total species involved in weathering reactions. These observations allow insights into naturally occurring geochemical processes in a pristine environment, while also providing baseline data for future research assessing the impacts of anthropogenic pollution and the effects of climate change.

Keywords: Clearwater Mesa, Geochemistry, Pristine environments, Major and trace elements, PHREEQC Modelling, High Latitude Lakes.

1. Introduction

Antarctica is home to some of the most pristine freshwater habitats remaining on Earth, and have intrigued scientists since the turn of the 20th century with the 'heroic age' of Antarctic exploration (e.g. West and West 1911; Fritch 1912; Goldman 1970; Burton 1981; Hobbie 1984; Abollino et al., 2012; Nedbalová et al., 2013). Few areas of the world still exhibit comparably pristine water geochemistry (Meybeck 2005), and here the natural background levels of major and trace elements can still be determined without obvious indications of human perturbation, enhancing the worth of these localities for investigating natural processes in freshwater systems,

such as solute mixing and geochemical weathering (Healy et al., 2006; Wait et al., 2006; Lyons et al., 2012).

However, Antarctic freshwater systems are also rapidly changing due to a shifting climate and increased human activity, especially in the Peninsula region (e.g., Turner et al., 2009), thus making their investigation timely. Lakes in the Antarctic Peninsula have long been regarded as sensitive indicators of environmental changes suitable for ecological monitoring and climatic reconstructions through paleolimnological studies (e.g., Quayle et al., 2002; Toro et al., 2007; Verleyen et al., 2012; Lee et al., 2017). While significant progress in the study of these lakes has been made during the last several years with respect to geochemical processes (e.g., Silva-Busso et al., 2013; Vignoni et al., 2014; Lecomte et al., 2016; Vignoni et al., 2017), there is still much to learn about how the differences in geochemistry arise.

Recently, Roman et al. (2019) described the geomorphology and hydrological systems of a previously unexplored region of James Ross Island (JRI) near the tip of the Antarctic Peninsula, appropriately named 'Clearwater Mesa' (CWM). Interestingly, these lakes differ in their solute concentrations as a function of each waterbody's underlying geology, hydrologic connectivity, and proximity to the coast, and exhibit considerable variability even within relatively small distances between other sites (Roman et al., 2019). Given the unique geologic and hydrologic setting of CWM, as well as the role these interacting processes likely exert on resident flora and fauna (some of which are unique to the Antarctic Peninsula region, Kopalová et al., 2012; 2013; 2014; in press), CWM represents an important opportunity for hydrological and geochemical investigation.

In this study, we build upon work initiated in Roman et al. (2019) by identifying the sources of major and minor solutes, and characterize associated patterns in weathering to improve our knowledge of how Antarctic lacustrine environments are formed and have evolved.

Specifically, we compare the sedimentology, major, minor and trace element concentrations, and perform geochemical modelling between surficial drainage basins that differ in weathering patterns based on their spatial juxtaposition and connectivity with other waterbodies. The results of this work not only shed light onto the dominant weathering regimes that have likely taken place since the last glacial maximum/recession, but also provide data (including metal/oids) which can be used as a basis for inter-site comparisons (e.g., at other latitudes and regions of Antarctica), as well as baseline data for eventual monitoring programs to track the imminent physico-chemical transition of these lake systems to a new climate equilibrium.

2. Geological and climatic setting

The climate of JRI is influenced by the boundary between the continental and arid Weddell Sea sector of the Antarctic Peninsula and the more humid maritime sub-Antarctic air masses. The result is a semi-arid climate (Laity 2008) characterized by short summers (December–February), with annual snowfall ranging from 200 mm to 500 mm yr^{-1} water equivalent of precipitation (Van Lipzig et al., 2004) and mean temperatures for the warmest and coldest months at Marambio Station (64º14’ S, 56º38’ W) being -3.3 and -14.5 ºC, respectively. Most waterbodies were formed by glacial erosion and deposition on ice-free areas following ice cap retreat during the Holocene (e.g., Ingólfsson et al., 1998; Carrivick et al., 2012), and show particular characteristics as a result of annual freeze-thaw cycles, simple trophic structure, marine proximity, and geographic isolation.

CWM is an ice-free 8 km^2 volcanic mesa situated ~250 m a.s.l., in the southeast side of Croft Bay in James Ross Island, east of the northern tip of the Antarctic Peninsula (63º40’ – 64º20’ S and 57º00’ – 58º00’ W; Fig. 1). CWM lakes were formed over James Ross Island

Volcanic Group (JRIVG) rocks, composed mainly of alkaline basalts and palagonitized hyaloclastite breccias (Jones and Nelson 1970; Košler et al., 2009; Smellie et al., 2013), and covered by glacial deposits with basaltic clasts. More than 60 shallow lakes and ponds can be found on CWM, with surfaces varying from ~130 to ~850 m^2. A few lakes are found at lower altitudes, located in glacial deposit depressions or are ice-marginal lakes formed during the last glacial retreat after the Little Ice Age (Carrivick et al., 2012). An example is Lake Florencia, which is also thought to be the deepest, as suggested by the size of the glacier that it drains.

Depending on their nature and geomorphological position, lakes are fed by direct snow/ice melt, the active layer of the permafrost, and/or surface runoff as represented by small streams connecting lakes. This surface connectivity results in distinct surficial drainage systems, and Roman et al. (2019) recognized five different systems on CWM (Fig. 1), which we hypothesize to exhibit predictable characteristics in terms of geochemistry, weathering, and sediment structure. The biggest system, the Katerina system, includes 23 lakes that are connected through active streams, or belong to the same catchment area. Systems Trinidad-Tatana, Norma and Florencia, are smaller (Fig. 1). We have grouped the 'isolated lakes' since they are hypothesized to have similar patterns in hydrological connectivity (or a lack thereof), being end-members in their lack of hydrologic connectivity with other waterbodies.

3. Materials and methods

3.1. Sampling and analyses

In order to characterize weathering processes in the hydrological systems of CWM, we collected water and sediment samples from 35 different lakes and ponds between 15-29 January 2015. Two ice samples (i.e., Blancmange Glacier and Lake Natasha-ice), were also collected to

compare the geochemical signature of the glacier source, and to identify the effect of repeated freezing processes in lakes. In addition, a precipitated salt sample was also collected from the margin of Lake Andrea. Thus, 72 CWM samples were collected in total: 2 ice, 35 lake water, 34 lake sediment, and one salt sample. The sediment samples were collected with a clean plastic shovel and stored in plastic bags.

For lake water and ice, temperature, pH, redox potential, electrical conductivity, and total dissolved solids (TDS) were measured *in situ*. Redox potential and pH was measured with a Hach digital detector, while temperature, TDS, and conductivity were measured using a digital Hach conductivimeter. Alkalinity was measured as $CaCO_3$ by end point titration in the field, using a 0.16 N H_2SO_4 solution until pH = 4.5. For anions, major cations, and trace elements determination, samples were vacuum-filtered in the field with carefully clean syringes and 0.22 µm pore-size cellulose filters (HA-type, Millipore Corp.). An aliquot was stored in triple-rinsed polyethylene bottles at 4 ºC for the determination of chloride and sulphate by chemically suppressed ion chromatography with conductivity detection (Thermo, model Constametric 3500, with Dionex suppressor and IonPac AS22 Dionex column -4 x 250 mm- for anions). Another aliquot was stored in centrifuge tubes pre-cleaned with diluted HNO_3, and then acidified (pH < 2) with concentrated, redistilled and ultrapure HNO_3 (Sigma-Aldrich) for the analytical determination of major and trace elements by inductively coupled plasma-mass spectrometry (Activation Laboratories Ltd., Ancaster, Ontario, Canada). These water samples were analysed by Perkin Elmer Sciex ELAN 9000 ICP/MS, Perkin Elmer Nexion, Thermo icapQ or Agilent 7700. A blank and two water standards were run at the beginning and end of each group of 32 samples. A reagent blank was run at the beginning of the group, and every 10^{th} sample was run in duplicate. The results for major and trace elements were validated using NIST (National Institute of Standards and Technology) 1640 and Riverine Water Reference Materials for Trace Metals

certified by the National Research Council of Canada (SRLS-4), and detection limits are reported in the corresponding tables. The accuracy (using standard ISO 17025) ranged between 1% and 10% in most cases. Additionally, duplicate analyses were performed to check the reproducibility of results, and precision was <9% for all analysed elements.

3.2. Sediment analysis

In order to examine weathering patterns and energy transfer within and between drainage basins as revealed by sediment composition and size structure, sediment samples were collected from the top 2-3 cm of the lake margins, with particular attention paid to the sediment/water interface. In total, 32 lakes were sampled, and the largest lake, Katerina, was sampled three times along its length to better characterize its spatial variability. Total organic and inorganic carbon (TOC and TIC, respectively) were determined for the bottom lake sediments and marginal salt samples to characterize particulate carbon distribution, and were estimated using the loss on ignition method (LOI; Heiri et al., 2001).

Sediment texture was determined with a particle analyser (Horiba LA-950), and samples were processed beforehand to remove any organic and inorganic content that could act as an agglomerating agent for the smallest grains, which would cause analytical error. Briefly, ~5 g of each sample was placed in a 50 ml centrifuge tube and reacted with sodium hexametaphosphate ($(NaPO_3)_6$) for 24 h to achieve clay defloculation. After the reaction, samples were washed with distilled water and centrifuged at 3500 R.P.M. for 5 min. This process was repeated four times for each sample. Hydrogen peroxide (30% H_2O_2) was then added to remove organic matter, and samples were washed again. Finally, samples were treated with 10% HCl for 120 h (5 days) to eliminate carbonates, followed by a final washing. In this case, the accuracy of measurements were <5%.

178 *3.3. Geochemical modelling*

179 Chemical data were processed with PHREEQC (Parkhurst 1995), constructed using the
180 AQUACHEM PHREEQC interface, to evaluate geochemical dynamics. To analyse lake
181 chemistry and evolution, these programs were used to perform several inverse and mixture
182 models for a small subset of lakes representing common routes of surface hydrologic
183 connectivity on CWM. Geochemical modelling simulates the interaction of cations and anions as
184 a function of temperature, redox potential, pH, and ionic strength. Inverse modelling was
185 performed to quantify weathering processes occurring first between connected snowmelt lakes
186 Esther and Tatana (due to being connected within a short distance, but exhibiting differences in
187 conductivity values), and second, between Blancmange Glacier and Lake Florencia. Lake
188 Florencia is a glacier-contact lake, in which dissolved chemistry is primarily controlled by
189 meltwater inputs emanating from the Blancmange Glacier. However, Lake Florencia also
190 receives water from the more concentrated Lake Cecilia via a small stream, though the extent to
191 which this input can influence the chemical make-up of Lake Florencia is uncertain.

192 Inverse modelling was conducted following the same methodology as Parkhurst and Apello
193 (1999) and Lecomte et al. (2005). Moreover, three mixing models with different proportions of
194 each solution were created to simulate mixing processes between sources. Models were
195 performed in equilibrium with $O_{2\,(g)}$ due to these being surficial hydrological systems.

196

197 **4. Results and Discussion**

198 *4.1. Hydrochemistry*

199 Table A.1 shows the area, and location of the studied lakes (adapted from Roman et al.,
200 2019), as well as the major physico-chemical variables and major ion concentrations determined

for the 37 lake water and ice samples from this work. Table A.2 presents the statistical values for each hydrogeological system's. In CWM lakes, the cationic and anionic order of abundance is the same as that reported in other Antarctic lake waters (e.g., Terra Nova Bay, Abollino et al., 2004). The analysed lakes were neutral to alkaline, with pH ranging between ~7.2 and ~9.4. Mildly alkaline waters are commonly associated with Ca-Mg carbonates (Deocampo and Jones 2014). Oxidizing conditions in the area are represented by Eh values between 263 and 412 mV, whereas the TDS content is highly variable, from <100 to □2250 mg L^{-1}. Conversely, both ice samples were diluted, slightly acid (pH □6.5), and present higher Eh values.

In the Katerina system, pH and conductivity values increased from the marginal lakes to those that receive the water from the streams connecting them (internal lakes). This suggests that weathering processes raise the dissolved element concentrations in the flow direction, with TDS ranging between 91.2 and 326 mg L^{-1} (lakes Susan and Linda, respectively), and pH values slightly alkaline to alkaline, between 7.8 and 9.2 (mean ~8.6). However, Trinidad-Tatana system's lakes show an increase in pH values related to a decrease in TDS. This system shows the highest pH, reaching 9.43 in Lake Esther and diminishing towards Lake Trinidad to a pH of 8.85. Norma system waters are more diluted (TDS values of ~150 mg L^{-1}), and pH is slightly alkaline. In the Florencia system, the homonymous lake exhibits the most diluted and circumneutral water among lakes (TDS 76.7 mg L^{-1}, pH 7.22) in the study area. The ice sample (from Blancmange Glacier) shows a low pH and extremely low TDS values (6.4 and 5.9 mg L^{-1} respectively). Finally, the remaining lakes on CWM are the outlying waterbodies (i.e. the 'isolated lakes'), and as they are not surficially connected, their physico-chemical parameters are highly variable (Table A.1).

White salt deposits were observed along the margins of lakes with high conductivity values (>1000 µS cm^{-1}). This results from evaporation processes combined with capillary flow that leads

to oversaturation in the lakes margin areas, resulting in mineral precipitation (e.g., Lecomte et al., 2016). Within the different hydrogeochemical environments defined according to the relationship between pH vs. Eh (Fig. A.1a, Baas Becking et al., 1960), the waters studied are clearly represented in the field between a transitional environment and surface waters.

Water ionic classification is shown in Fig. A.1b with a Piper diagram (Piper 1944), which is a plot that visually separates lakes according to their major ion chemistry. Cations (Ca^{2+}, Na^{+} + K^{+}, Mg^{2+}) and anions (Cl^{-}, SO_4^{2-}, HCO_3^{-} + CO_3^{2-}) are plotted in separate ternary diagrams according to their percentage values. Then, all ions are combined into one rhomboidal diagram showing their relative concentrations to visually infer the "type" of water and its main composition. Lake waters from CWM show a tendency from the most chloride type in the Florencia system, to the bicarbonate type mostly represented by the Katerina system. In the cationic triangle, water samples are sodic-potasic to mixed types, with little calcium contributions except for Lake Florencia, which is the only calcic-type sample. Moreover, ice melting from the Blancmange glacier that feeds Lake Florencia shows a different composition, being of the bicarbonate-sodic-potasic type. The other ice sample corresponds to Lake Natasha, being classified as bicarbonate-mixed type, whereas Lake Natasha is chloride-mixed type. Overall, CWM water follows a straight line, indicating the relative scarcity of SO_4^{2-} and Ca^{2+}. This pattern is similar to other lakes in JRI and Vega Island, and in streams, groundwater, and snow and ice on Fildes Peninsula (Ye et al., 2018), whereas lakes from Marambio Island are clearly sulphated waters (Lecomte et al., 2016).

4.2 Bottom Lake Sediments

4.2.1 Organic and inorganic carbon in lake sediments

Organic matter content (expressed as TOC) in surface sediment samples ranged from 0.82 to 4.81%, with an outlier of 14.26 represented by one of the three Katerina sediment samples (Table A.1; Fig. 2). The greatest values were recorded in sediment samples from Katerina and Andrea lakes, and can be explained by greater abundances of microbial mats, which were observed in most of the lakes, and are likely also related to high pH values through their photosynthesis (Chaparro et al., 2014). While there was no discernible pattern in TOC content between the different drainage systems, TOC increased within Lake Katerina from the northeast to the northwest coast (2.49 to 14.26).

Total inorganic carbon (TIC) content was relatively low in all samples, with values <1% (Table A.1). This can be observed in Fig. 2, with values compared with lakes from other nearby Antarctic islands (i.e., shaded areas, modified from Lecomte et al., 2016). The sample of precipitated salts has the highest TIC value (1.24%) due to evaporative processes, which decreases lake levels and consequently concentrates dissolved elements, and is generally accompanied by the precipitation of salts such as carbonates and sulphates. Thus, like for other nearby Antarctic islands (Lecomte et al., 2016), the lakes of CWM have low levels of carbonate production, and it can be assumed that the inorganic siliciclastic fraction constitutes the main component of sediments.

4.2.2. Granulometric size distribution

Sediment samples were analysed for their particle size distribution. High variability was observed among samples, with medium fractions (silts and fine sands) generally predominating. To improve visualization, the textures are represented in granulometric curves in which the diameter (µm) versus the percentage content of each grain size (q%) is plotted (Fig. 3). From

these plots, samples are clearly separated according to similar grain size patterns (bimodal and trimodal).

Fig. 3a shows a homogeneous bimodal granulometric distribution, corresponding to fine silts, while the second peak corresponds with very fine sands. Samples with a trimodal grain size distribution were divided into two groups according to the predominant main fraction: silts and sands (Fig 3b and c, respectively). The main peak in this first group corresponds with fine to very fine silts, while the second peak corresponds to fine sands, and the last peak to coarse sands. On the other hand, in the second group, the main peak corresponds to medium to coarse sands, while the middle peak corresponds to fine to very fine sands, and the smaller fraction represents fine to very fine silts (the salt sample is included in this group).

A Folk Diagram, which is used in the textural classification of sediments, is presented in Fig. 3d for sediments with <10% particles of gravel size (>2 mm). Size distributions of gravel-free sediments are plotted on a triangular diagram, where the three end-members are clay, silt, and sand. Locations and boundaries within the triangle reflect the two dimensions of silt/clay ratio and % sand. The relative proportion of the grains in the three categories is used to describe the sediment and classify it into ten textural classes. Most of the lakes don't present gravel content, whereas in only a few samples, this content ranges from 0.3% to 2.2%. Lake Cecilia is the only one with >10% (i.e., 12.5%) sediment >2 mm, implying that this lake cannot be classified under the Folk nomination scheme.

From a general point of view, the external lakes that drain into the internal lakes show a higher grain size with sandy samples, whereas the internal lakes present a higher percentage of silts and clays, accompanied by the increased TDS described in section *4.1.* (e.g., Valentina-Paula-Nora; Ludmila-Linda-Graciela). This evidences decreasing transport energy in the flow direction. Lake Katerina lends more support to this explanation: three samples were taken from

295 the northeast to the northwest coast (Fig. 1), and present increasing TOC values (as was indicated
296 in section 4.2.1) and clay content (which increases from 2.6 to 16.3%), whereas the sand and silt
297 content decreases in the same direction. The decrease in granulometric size, along with the
298 increasing of TOC values in the flow direction, indicate lower transport energy towards the
299 northwest coast.
300
301 *4.3. Dissolved trace element behaviour*
302 The trace element concentration of each water and ice sample is presented in Table B.1 and
303 Table B.2. In order to evaluate their areal distribution, dissolved concentrations were normalized
304 to the upper continental crust (UCC, McLennan 2001) and results are shown in a spidergram
305 (Fig. B.1). Water samples from surface hydrological systems show between 10^{-3} to 10^{-7} lower
306 concentrations that the regional basalts. As expected, those elements which exhibit higher relative
307 concentrations are those that are more labile, being more stable in the dissolved phase in
308 exogenous conditions instead of in the solid one (i.e., mineral). In contrast, for high field strength
309 (HFS) elements, UCC-normalized concentrations were $<10^{-6}$ in most cases (i.e., Al, Fe, Ti, Ba,
310 Zr, Y, Th, and Hf). The HFS elements have a small radius compared to their high cationic charge
311 (i.e., the z/r ratio), and as a result, their bonding to nearby anions is very strong, restricting their
312 mobility.
313 The world average geochemical composition (Gaillardet et al., 2014) was added to plots for
314 comparison, being in the range of CWM samples in general. However, it is interesting that some
315 elements in CWM lakes present higher concentrations than the world average (i.e., Ti, Zn, Pb),
316 whereas others are lower (i.e., Mn, Ba, Sr, Rb, Th). These lower concentrations are controlled by
317 water-bedrock interactions, and most of these elements are associated with acid rocks, such as
318 granitoids, but are comparatively depleted in volcanic rocks. When comparing with other nearby

Antarctic lakes, the similarity of trace element concentrations in CWM with lakes from Vega Island is evident, although concentrations are lower than lakes from Marambio Island and JRI (Lecomte et al., 2016).

The mean JRIVG geochemical composition of basaltic lava flows, dykes and breccias was calculated according to values reported by Košler et al. (2009), and was also added to Fig. B.1 and Table B.1. These rocks clearly show a depletion of alkali elements and an enrichment of some metals (e.g., V, Cr, Cu, Ni, Sc, Co) common in alkaline basalts, explaining trace element distributions. However, Pb and Zn exhibit substantial enrichment (Fig. B.1), which can be related not only with mineral weathering but also with atmospheric contamination, as has been deduced in the Northern Hemisphere by Murozumi et al. (1969), and in the Arctic and Antarctic regions by Boutron et al. (1987); Hong et al. (1998); and Planchon et al. (2002).

4.5. Geochemical dynamics

In order to recognize the influence of sea spray in lake water geochemistry, Mg^{2+}/Ca^{2+} and $Na^{+}/(Na^{+}+Ca^{2+})$ meq L^{-1} ratios were calculated, as well as the relationship of Na^{+} vs Cl^{-}. Mg^{2+}/Ca^{2+} ratio values (Table A.1) ranged from 0.03 to 12.86, with an average value of ~3. $Na^{+}/(Na^{+}+Ca^{2+})$ ratio values ranged from 0.09 to 0.93, with an average of ~0.8. The minimum values both belonged to Lake Florencia, while the maximum values were calculated for Lake Adriana. These results can potentially be explained by the lake's distance to the sea, its hydrologic connectivity, and/or its geomorphological position (Roman et al., 2019). Lake Florencia is located in a depression formed on one side by a glacier and being protected from sea influence, while Lake Adriana is located in the southern part of the mesa, hydrologically isolated and close to the cliff edge. In a general way, lakes located to the east in the Nuñez Valley show lower ratios due to the increasing distance to the sea and the presence of geomorphological

343 barriers. On the other hand, lakes located on the west side of the mesa near the cliff edge exhibit
344 the greatest ratio values as a consequence of sea spray, as evidenced by the high correlation
345 between Na^+ and TDS, reaching $R^2 = 0.96$. The relationship between Na^+ and Cl^- resulted in an
346 $R^2 = 0.77$, corroborating the atmospheric source, whereas Ca^{2+} and Mg^{2+} concentrations in lake
347 water can be also derived from the weathering of plagioclases and ferromagnesian minerals
348 present in the basaltic rocks and breccias that constitute the lake's basement.

349 Because of low temperatures and arid conditions, the main geochemical processes
350 controlling dissolved concentrations are atmospheric spray and evaporation. However, chemical
351 weathering and many other water-based rock decay processes are also present to a different
352 extent. In order to characterize those weathering processes, inverse modelling was performed
353 between Esther and Tatana samples, which are connected to each other via a surficial stream.
354 Modelling results approximate the system's behavior, seeking an estimate to the amount of moles
355 transferred between the dissolved, gaseous, and solid phases. Appendix C shows the output of the
356 geochemical model, whereas Table 1 summarizes the results. The processes occurring between
357 lakes are: the dissolution between 0.1 and up to 5.1 mmol L^{-1} H_2O of plagioclase, feldspar,
358 muscovite, dolomite, salts, and a significant consumption of CO_2 by weathering reactions. On the
359 other hand, between 0.5 and 1.2 mmol L^{-1} H_2O of calcite and illite precipitate.

360

361 *4.6. Lake Florencia's water source(s)*

362 Lake Florencia receives water from the Blancmange Glacier, but also from a stream
363 draining Lake Cecilia. To estimate the potential contribution of these sources, as well as to assess
364 the potential role of weathering processes in generating the final chemical composition of Lake
365 Florencia, mixing models were created with different source proportions in an exploratory
366 manner (i.e., one model where both the glacier and stream contribute 50% of the water, one

where 20% of the water is from the glacier and 80% is from Lake Cecilia, and one where 80% of the water is from the glacier and 20% is from Lake Cecilia). Results are shown in Fig. 4a, and the best fitting model is the last one (i.e., green spots in Fig. 4), which indicates a smaller influence of the stream draining Lake Cecilia and a much greater likely contribution of meltwater from the glacier. However, it is clear that additional weathering processes are still necessary to adequately explain the dissolved concentrations of this lake. Lake Florencia's TDS value is intermediate between both sources, being the highest in Lake Cecilia. It means that between both lakes, there is no possibility of weathering processes that increase dissolved ions, as on the contrary, mineral precipitation should occur due to the lower TDS values. One possibility may be that some weathering processes may be acting at the base of the glacier as explained by Lorrain and Fitzsimons (2011), which modifies the hydrochemical signal.

The partial melting of permafrost in summer could also provide a solution to balancing the lake's hydrochemistry. From this interpretation, inverse modelling was performed to quantify the potential geochemical processes, and with these results, it is possible to explain Lake Florencia's hydrochemistry (Fig. 4b). The model was chosen considering JRIVG mineralogy. Specifically, these basalts present high amounts of calcite filling holes and amygdala, and plagioclases are more sodic than calcic. Uncertainties were 5% for the Blancmange Glacier sample and 2% for Lake Florencia. Silicate weathering transfers 1.1 10^{-2} mmol L^{-1} H_2O to the dissolved phase, whereas carbonate weathering removes 1.9 10^{-2} mmol L^{-1} H_2O. Mineral weathering transfers 1.2 10^{-1} mmol L^{-1} H_2O to the dissolved phase consuming 5.4 10^{-5} mmol L^{-1} H_2O of CO_2, with the corresponding generation of 1.3 10^{-2} mmol L^{-1} H_2O of residual clays. The minerals which explain weathering are: albite, muscovite, calcite, dolomite, gypsum, halite, and kaolinite.

5. Final remarks

391 The present study contributes baseline data to help better understand weathering processes
392 influencing the hydrochemistry of Antarctic lakes. Specifically, by studying different lake
393 systems located on CWM, our results allow for a characterization of mechanisms responsible for
394 their physical and chemical attributes. Although CWM is only 8 km^2, it contains more than 50
395 lakes and ponds that constitute connected lake systems, as well as isolated lakes with different
396 physico-chemical characteristics. Most of the lakes have dilute alkaline waters, except for the
397 isolated basin ones that exhibit higher concentration waters and salt precipitation in their margins
398 due to evaporative processes.

399 Low temperatures, arid conditions, and high wind velocity enhances evaporation processes
400 and the influence of atmospheric spray. The major element composition of CWM lakes reflects
401 the significant influence of marine spray in the water chemistry, varying according to the distance
402 to the sea, lake geomorphological position, and melt-water input during the austral summer (see
403 also Roman et al., 2019). However, the influence of chemical weathering in this extreme
404 environment must not be ignored, as evidenced by our modelling exercises. Chemical weathering
405 contributes to the major ionic composition, as it results in the release of the most labile elements
406 during the weathering process, such as Ca^{2+}, Na^{+}, K^{+}, and Mg^{2+}. Through our analyses, we found
407 that the processes occurring in the drainage basins include the dissolution of plagioclase, K-
408 felspar, muscovite, calcite, dolomite, halite and gypsum, the precipitation of illite or kaolinite,
409 and a significant consumption of CO_2 by weathering reactions. Between 10^{-3} and 10^{-1} mmol L^{-1}
410 H_2O of different phases are dissolved or precipitated in the reactions.

411 By separating the lakes into their surficial drainage systems, we found that these different
412 lake systems exhibit weathering patterns through their ‘external’ to ‘internal’ lakes. For example,
413 lakes with lower sediment grain size (and higher TOC values) reflect the lower energy states, and
414 were found more in the more internal waterbodies. Although overall the sediments are mainly

415 composed of silts and sands, the clay fraction represents the most reactive one in terms of water-
416 sediment interactions/surface availability for absorption processes.

417 Minor and trace metal concentrations in CWM lakes are controlled by water-sediment and
418 water-bedrock interactions, as well as surface water input. Trace elements that present high-
419 normalized concentrations compared to the world average (Cr, Cu, Ni, Sc, Co) correspond to
420 metals that are enriched in JRIVG rocks, therefore reflecting their main source. Collectively,
421 these results provide important insights into geochemical processes taking place in high-latitude
422 lakes and ponds, which are important given that the release of weathering products to the
423 surrounding terrestrial and aquatic areas could play an important role in species distributions and
424 overall ecosystem health.

425

426 **Declaration of interest**

427 None.

428

429 **Acknowledgments:** The authors wish to thank Dirección Nacional del Antártico (DNA), and
430 Instituto Antártico Argentino (IIA) for the financial and logistical support in Antarctica. This
431 work was supported by Agencia Nacional de Promoción Científica y Tecnológica (ANPCYT
432 projects PICTO-2010-0096 and PICT 2017-2026); by the Consejo Nacional de Investigaciones
433 Científicas y Técnicas (CONICET, Argentina, projects PIP 11220170100088CO and PUE-
434 CICTERRA 2016); and by the Universidad Nacional de Córdoba (SeCyT, project 336-
435 20180100385-CB). Funding was also provided by the Ministry of Education, Youth and Sports
436 of the Czech Republic projects LM2015078 and CZ.02.1.01/0.0/0.0/16_013/0001708, and the
437 Masaryk University project MUNI/A/1576/2018. Authors TJK and KK were further supported by
438 Charles University Research Centre program No. 204069.

439

440 **References:**

441 Abollino, O., Aceto, M., Buoso, S., Gasparon, M., Green, W.J., Malandrino, M., Mentasti, E.,
442 2004. Distribution of major, minor and trace elements in lake environments of Antarctica. Antarc.
443 Sci. 16, 277-291. DOI: 10.1017/S0954102004002111

444 Abollino, O., Malandrino, M., Zelano, I., Giacomino, A., Buoso, S., Mentasti, E., 2012.
445 Characterization of the element content in lacustrine ecosystems in Terra Nova Bay, Antarctica.
446 Microchem. J. 105, 142-151.

447 Baas Becking, L.G.M., Kaplan, I.R., Moore, D., 1960. Limits of the natural environment in terms
448 of pH and oxidation-reduction potentials. J. Geol. 68, 243–284.

449 Bargagli, R., 2005. Antarctic Ecosystems. Environmental Contamination, Climate Change, and
450 Human Impact. ISBN 3-540-22091-7 Springer-Verlag, Berlin, Heidelberg, New York.

451 Boutron, C. F., Patterson, C. C., Petrov, V. N., and Barkov, N. I., 1987. Preliminary data on
452 changes of lead concentrations in Antarctic ice from 155,000 to 26,000 years BP, Atmos.
453 Environ. 21, 1197– 1202.

454 Burton, H. R., 1981. Chemistry, physics and evolution of Antarctic saline lakes. Hydrobiologia
455 82, 339–362.

456 Carrivick, J.L., Davies, B.J., Glasser, N.F., Nývlt, D., 2012. Late Holocene changes in character
457 and behaviour of land-terminating glaciers on James Ross Island, Antarctica. J. Glaciol. 58,
458 1176-1190.

459 Chaparro, M.A.E., Gargiulo, J.D., Irurzun, M.A., Chaparro, M.A.E., Lecomte, K.L., Böhnel,
460 H.N., Córdoba, F.E., Vignoni, P.A., Manograsso, N.T., Lirio, J.M., Nowaczyk, N.R., Sinito,
461 A.M., 2014. El uso de parámetros magnéticos en estudios paleolimnológicos en Antártida
462 "Magnetic parameters in paleolimnological studies in Antarctica". Lat. Am. J. Sedimentol. Basin
463 Anal. 21,77-96.

464 Deocampo, D.M. and Jones, B.F., 2014. Geochemistry of saline lakes, in: Drever, J.I. (Ed.),
465 Surface and Groundwater, Weathering and Soils, Treatise on Geochemistry, 2nd ed., Elsevier,
466 Amsterdam, 7, pp. 437-469.

467 Folk, R.L., 1974. Petrology of Sedimentary Rocks. Hemphill, Austin, Texas, pp. 1-57.

468 Fritsch, F.E., 1912. Freshwater Algae. National Antarctic "Discovery" Expedition 1901–1904.
469 British Museum of Natural History 6, 1-66.

Gaillardet, J., Viers, J., & Dupré, B., 2014. Trace Elements in River Waters, in: Holland, H.D. and Turekian K.K. (Eds.), Treatise on Geochemistry, 2nd ed., Elsevier, Oxford, 7.7, pp. 195-235.

Goldman, C. R., 1970. Antarctic Fresh-Water Ecosystems. In: Holdgate, M. W. (Ed.) Antarctic Ecology, Academic Press, NY, pp. 609–627.

Healy, M., Webster-Brown, J.G., Brown, K.L. and Lane, V., 2006. Chemistry and stratification of Antarctic meltwater ponds II: Inland ponds in the McMurdo Dry Valleys, Victoria Land. Antarc. Sci. 18, 525-533.

Heiri, O., Lotter, A.F., Lemcke, G., 2001. Loss on ignition as a method for estimating organic and carbonate content in sediments: reproducibility and comparability of results. J. Paleolim. 25,101–110.

Hobbie, J. E., 1984. Polar Limnology, in: Taub, F.B. (Ed.), Lakes and Reservoirs. Elsevier, Amsterdam, pp. 63–105.

Hong, S., Boutron C.F., Edwards, R., Morgan V.I., 1998. Heavy metals in Antarctic ice from Law Dome: initial results. Environ. Res., 78, 94-103.

Ingólfsson, O., Hjort, C., Berkman, P., Björck, S., Colhoun, E., Goodwin, I.D., Hall, B., Hirakawa, K., Melles, M., Möller, P., Prentice, M., 1998. Antarctic glacial history since the Last Glacial Maximum: an overview of the record on land. Antarc. Sci. 10, 326-344.

Jones, J.G. and Nelson, P. H. H., 1970. The flow of basalt lava from air into water - its structural expression and stratigraphic significance. Geol. Mag. 107, 13-19.

Kopalová, K., Elster, J., Komárek, J., Veselá, J., Nedbalová, L., Van de Vijver, B., 2012. Benthic diatoms (Bacillariophyta) from seepages and streams on James Ross Island (NW Weddell Sea, Antarctica). Plant. Ecol. Evol. 145,190-208.

Kopalová, K., Nedbalová, L., Nývlt, D., Elster, J., Van de Vijver, B., 2013. Diversity, ecology and biogeography of the freshwater diatom communities from Ulu Peninsula (James Ross Island, NE Antarctic Peninsula). Polar Biol. 36, 933-948.

Kopalová, K., Ochyra, R., Nedbalová, L., Van de Vijver, B., 2014. Moss inhabiting diatoms from two contrasting Maritime Antarctic islands. Plant. Ecol. Evol. 147, 67-84.

Kopalová, K., Soukup, J., Kohler, T.J., Roman, M., Coria, S.H., Vignoni, P.A., Lecomte, K.L., Nedbalová, L., Nývlt, D., Lirio, J.M. In press. Habitat controls on limno-terrestrial diatom communities of Clearwater Mesa, James Ross Island, Maritime Antarctica. Polar Biol. doi.org/10.1007/s00300-019-02547-8.

Košler, J., Magna, T., Mlcoch, B., Mixa, P., Nýlt, D., Holub, F.V., 2009. Combined Sr, Nd, Pb and Li isotope geochemistry of alkaline lavas from northern James Ross Island (Antarctic Peninsula) and implications for back-arc magma formation. Chem. Geol. 258, 207–218.

Laity, J. 2008. Deserts and desert environments. Wiley-Blackwell, Chichester, UK.

Lecomte, K.L., Pasquini, A.I., Depetris, P.J., 2005. Mineral weathering in a semiarid mountain river: its assessment through PHREEQC inverse modeling. Aquatic Geochem. 11, 173–194.

Lecomte, K.L., Vignoni, P.A., Córdoba, F.E., Chaparro, M.A.E., Chaparro, M.A.E., Kopalová, K., Gargiulo, J.D., Lirio, J.M., Irurzun, M.A., Böhnel, H.N., 2016. Hydrological systems from the Antarctic Peninsula under climate change: James Ross archipelago as study case. Environ. Earth Sci. 75, 1-20. DOI:10.1007/s12665-016-5406-y

Lee, J. R., Raymond, B., Bracegirdle, T. J., Chadès, I., Fuller, R. A., Shaw, J.D., Terauds, A., 2017. Climate change drives expansion of Antarctic ice-free habitat. Nature, 547, 49–55.

Lorrain R.D., Fitzsimons S.J., 2011. Cold-Based Glaciers. In: Singh V.P., Singh P., Haritashya U.K. (Eds) Encyclopedia of Snow, Ice and Glaciers. Encyclopedia of Earth Sciences Series. Springer, Dordrecht.

Lyons, W.B., Welch, K.A., Gardner, C.B., Jaros, C., Moorhead, D.L., Knoepfle, J.L., Doran, P.T., 2012. The geochemistry of upland ponds, Taylor Valley, Antarctica. Antarct Sci. 24, 3–14. doi:10.1017/S0954102011000617

McLennan, S.M., 2001. Relationships between the trace element composition of sedimentary rocks and upper continental crust. Geochem. Geophys. Geosyst. doi:10.1029/2000GC000109

Meybeck, M., 2005. Global Occurrence of Major Elements in Rivers, in: Drever J.I. (Ed.), Surface and ground water, weathering, and soils. Elsevier, Amsterdam, 5, pp. 207-223.

Murozumi, M., Chow, T.J., and Patterson, C.C., 1969, Chemical concentration of pollutant lead aerosols, terrestrial dusts and sea salts in Greenland and Antarctic snow strata: Geochim. Cosmochim. Acta, 33, 1247-1294.

Nedbalová, L., Nývlt, D., Kopáček, J., Šobr, M. and Elster, J., 2013. Freshwater lakes of Ulu Peninsula, James Ross Island, north-east Antarctic Peninsula: origin, geomorphology and physical and chemical limnology. Antarct. Sci. 25, 358-372.

Parkhurst, D. L., 1995. User's guide to PHREEQC-A computer program for speciation, reaction-path, advective-transport, and inverse geochemical calculations. U.S. Geol. Surv. Water Res. Invest. Rep. 95- 4227.

Parkhurst, D.L. and Apello, C.A., 1999. User´s guide to PHREEQC (versión 2) – a computer code program for speciation, bathreaction, one- dimensional transport and inverse geochemical calculations. U.S. Geol. Surv. Water Res. Invest. Rep. 99-4259.

Piper, A.M., 1944. A graphic procedure in the geochemical interpretation of water analyses. Trans. Am. Geophys. Union 25, 914-923.

Planchon, F.A.M., Boutron, C.F., Barbante, C., Cozzi, G., Gaspari, V., Wolff, E.W., 2002. Changes in heavy metals in Antarctic snow from Coats Land since the mid-19th to the late-20th century. Earth Planet Sci. Lett. 200, 207-222.

Quayle, W.C., Peck, L.S., Peat, H., Ellis-Evans, J.C., Harrigan, P.R., 2002. Extreme responses to climate change in Antarctic lakes. Science 295:645.

Roman, M., Nedbalová, L., Kohler, T., Lirio, J., Coria, S., Kopáček, J., Vignoni, P.A., Kopalová, K., Lecomte, K.L., Elster, J., Nývlt, D., 2019. Lacustrine systems of Clearwater Mesa (James Ross Island, north-eastern Antarctic Peninsula): Geomorphological setting and limnological characterization. Antarct. Sci. 31(4): 169-188. doi:10.1017/S0954102019000178

Silva –Busso, A., Moreno, L., Ermolin, E., López-Martínez J., Durán, J.J., Martínez-Navarrete C., Cuchí, J.A., 2013. Modelos hidrogeológicos a partir de datos geocriológicos e hidroquímicos en Cabo Lamb, Isla Vega, Península Antártica. RAGA. 70:249-266.

Smellie, J.L., Johnson, J.S. and Nelson, A.E., 2013. Geological map of James Ross Island. I. James Ross Island Volcanic Group (1:125 000 scale). BAS GEOMAP 2 Series, Sheet 5, British Antarctic Survey, Cambridge, UK.

Toro, M., Camacho, A., Rochera, C., Rico, E., Bañón, M., Fernández-Valiente, E., Marco, E., Justel, A., Avendaño, M.C., Ariosa, Y.,Vincent, W.F., Quesada, A., 2007. Limnological characteristics of the freshwater ecosystems of Byers Peninsula, Livingston Island, in maritime Antarctica. Polar Biol. 30, 635-649.

Turner, J., Bindschadler, R., Convey, P., di Prisco, G., Fahrbach, E., Gutt, J., Hodgson, D., Mayewski, P., Summerhayes, C., 2009. Antarctic Climate Change and the Environment. Scientific Committee on Antarctic Research Scott Polar Research Institute, Lensfield Road, Cambridge, UK. ISBN 978-0-948277-22-1, pp. 555.

Van Lipzig, N.P.M., Turner, J., Colwell, S.R., Van Den Broeke, M.R., 2004. The near-surface wind field over the Antarctic Continent. Int. J. Climatol. 24, 1973-1982.

Verleyen, E., Hodgson, D.A., Gibson, J., Imura, S., Kaup, E., Hoshino, T., Kanda, H., Kudoh, S., De Wever, A., Hoshino, T., McMinn, A., Obbels, D., Roberts, D., Roberts, S.J., Sabbe, K., Souffreau, C., Tavernier, I., Van Nieuwenhuyze, W., Van Ranst, E., Vindevogel, N., Vyverman,

W., 2012. Chemical limnology in coastal East Antarctic lakes: monitoring future climate change in centres of endemism and biodiversity. Antarct. Sci. 24, 23–33.

Vignoni, P.A., Lecomte, K.L., Chaparro, M.A.E., Gargiulo, J.D., Chaparro, M.A.E., Kopalová, K., Córdoba, F.E., Irurzun, A., Lirio J.M., Urán, G., Gorosito, M., Cañas, E., 2014. Hydrochemical, sedimentological, biological and magnetic characterization of lakes in James Ross Archipelago, Antarctica. 3º Reunión Argentina de Geoquímica de la Superficie (3º RAGSU), Actas: 208–212, ISBN: 978-978-544-598-7, Mar del Plata, Argentina.

Vignoni, P.A., Lecomte, K.L., Lirio, J.M., Coria, S.H. Origen de elementos mayoritarios y caracterización de sistemas lacustres prístinos en Clearwater Mesa, Isla James Ross, Península Antártica. Artículo breve. XX Congreso Geológico Argentino, Tucumán 7-11 agosto 2017. ST:18, 122-128.

Wait, B.R., Webster-Brown, J.G., Brown, K.L., Healy, M. and Hawes, I., 2006. PChemistry and stratification of Antarctic meltwater ponds I: coastal ponds near Bratina Island, McMurdo Ice Shelf. Antarct. Sci. 18(4), 515-524.

West, W. and West, G.S., 1911. Freshwater algae. British Antarctic.

Ye, L., Zhang, R., Sun, Q., Jin, J., Zhang, J., 2018. Hydrochemistry of the meltwater streams on Fildes Peninsula, King George Island, Antarctica. J. Oceanol. Limn. 36, 2181-2193. doi.org/10.1007/s00343-019-7193-2

Figure captions

Fig. 1: Map of Clearwater Mesa, with different waterbodies labelled according to their surface hydrological drainage system.

Fig. 2: Percentage of Total Inorganic Carbon (%TIC) versus the percentage of Total Organic Carbon (%TOC) in sediment samples. Marambio, James Ross, and Vega islands data are represented as shaded areas and taken from Lecomte et al. (2016).

Fig 3: Sediment sample granulometric curves: a) bimodal; b) trimodal sand; c) trimodal silt; and d) ternary diagram showing textures of sediment samples (modified from Folk, 1974)

Fig. 4: PHREEQC modelling results, a) mixing modelling: scatter graph showing the relationship between Lake Florencia real dissolved chemistry concentration (mg L^{-1}) and a three modeled solution by mixing Blancmange Glacier (i.e., BG) and Lake Cecilia (i.e., LC) in different proportions. The y = x straight line of equal concentrations is included as a reference, b) inverse modelling: mmol L^{-1} H_2O of different transferred. Positive values are for dissolved phases and negative values are for precipitated ones.

Tables:

Table 1. PHREEQC inverse modelling results showing mmol L^{-1} H_2O of different transferred dissolved and precipitated phases. Both solution uncertainties and the model's sum of residuals are included.

Supplementary material:

Appendix A:

Table A.1. Physical and chemical variables from this study including sample locations, lake area, pH, conductivity, major ions, TIC, and TOC.

Table A.2. Statistical values for each hydrogeological system's physical and chemical characteristics.

Fig. A.1: a) pH-Eh diagram; b) Piper diagram from Clearwater Mesa lake and ice water samples.

Appendix B:

Table B.1. Trace element determined in the 2015 sampling campaing and JRIVG mean values (in ppm) are from concentrations reported by Košler et al., 2009.

Table B.2. Statistical values for each hydrogeological system's trace elements.

Fig. B.1: Upper Continental Crust normalized spidergram. The JRIVG average (Košler et al., 2009) and world average (Gaillardet et al., 2014) are added for comparison.

Appendix C: Inverse modelling results.

Table 1. PHREEQC inverse modelling results showing mmol L-1 H2O of different transferred dissolved and precipitated phases. Both solution uncertainties and the model's sum of residuals are included.

Inverse modelling	**Initial solution**	**Final solution**
	Esther	Tatana
uncertainty	0.08	0.05
Phases transferred	Dissolved	Precipitated
	mmol kg^{-1} H_2O	
CO2(g)	2.18	
Albite	0.27	
Calcite		-1.22
Dolomite	1.75	
Halite	5.08	
Illite		-0.47
K-feldspar	0.09	
Muscovite	0.24	
Gypsum	0.10	
sum of residuals	4.69	
fractional error in element concentration	0.05	

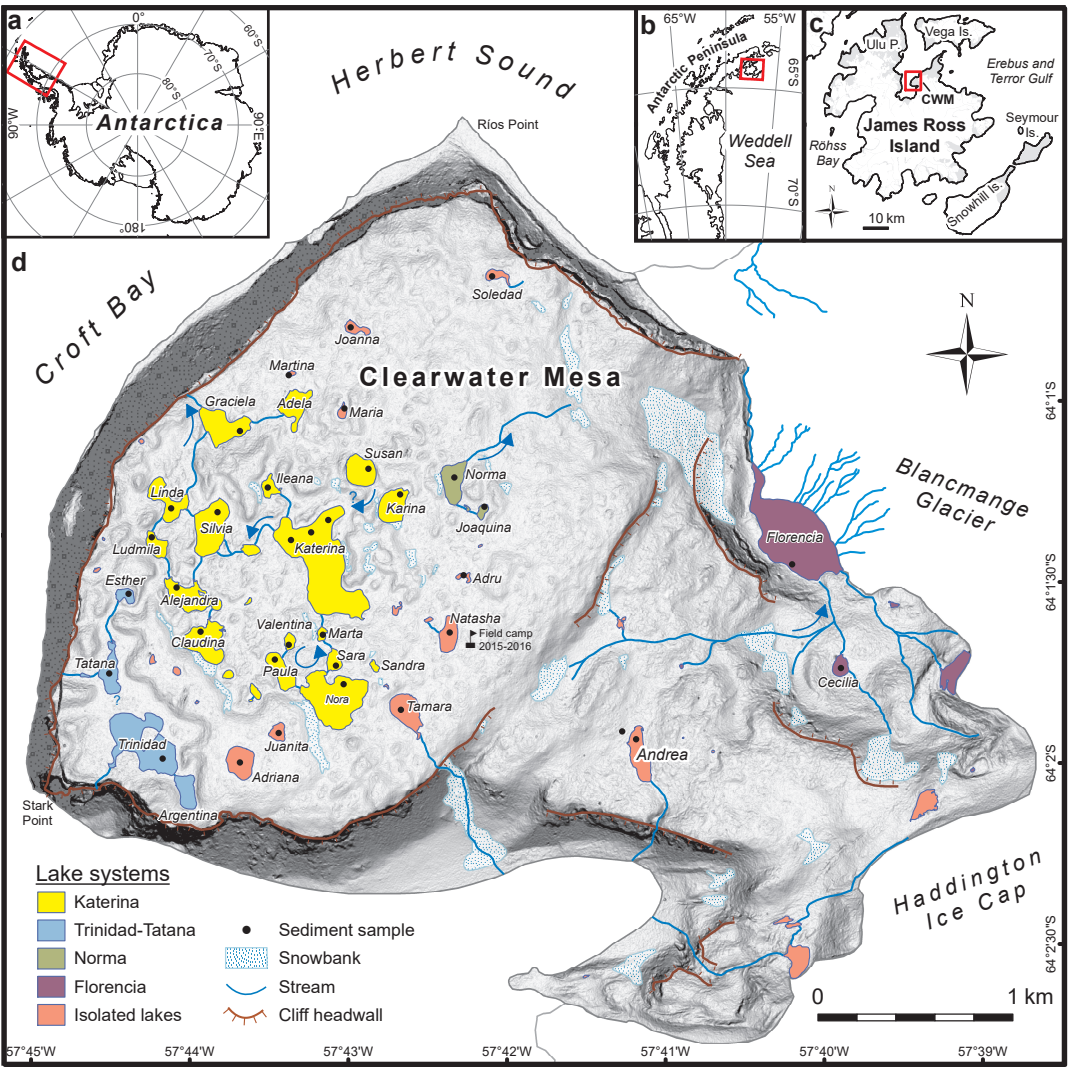
a
Antarctica
0°
60°S
70°S
80°S
90°W
90°E
180°
b
65°W
55°W
65°S
70°S
Antarctic Peninsula
Weddell Sea
c
Ulu P.
Vega Is.
Erebus and Terror Gulf
CWM
James Ross Island
Seymour Is.
Röhss Bay
Snowhill Is.
10 km
d
Herbert Sound
Ríos Point
Croft Bay
Clearwater Mesa
Soledad
Joanna
Martina
Graciela
Adela
Maria
Susan
Ileana
Norma
Linda
Karina
Joaquina
Silvia
Katerina
Ludmila
Florencia
Esther
Adru
Alejandra
Natasha
Field camp 2015-2016
Valentina
Marta
Claudina
Sara
Sandra
Tatana
Paula
Nora
Cecilia
Tamara
Trinidad
Juanita
Andrea
Adriana
Stark Point
Argentina
Blancmange Glacier
Haddington Ice Cap
N
Lake systems
Katerina
Trinidad-Tatana
Norma
Florencia
Isolated lakes
Sediment sample
Snowbank
Stream
Cliff headwall
0
1 km
64°1'S
64°1'30"S
64°2'S
64°2'30"S
57°45'W
57°44'W
57°43'W
57°42'W
57°41'W
57°40'W
57°39'W

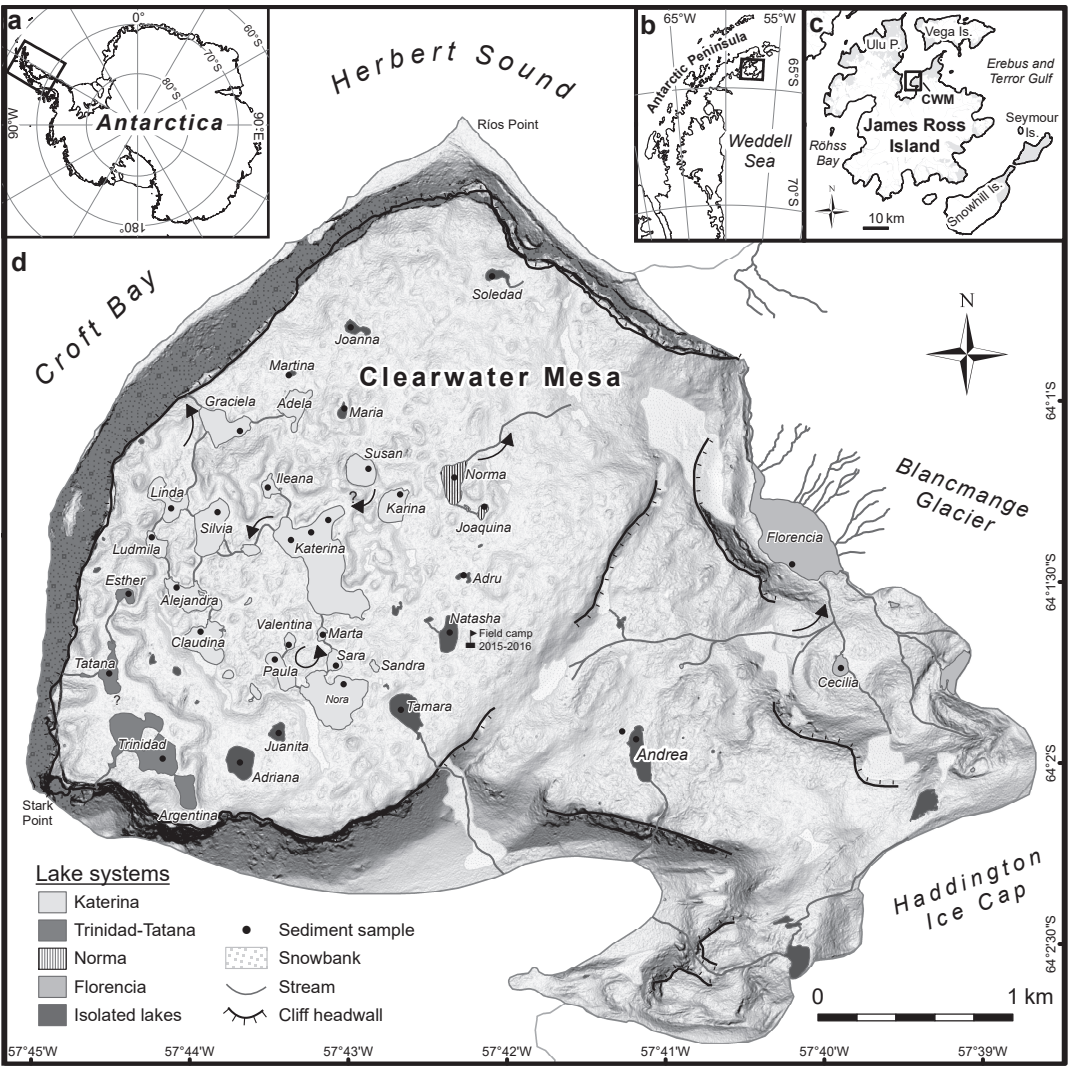
a
Antarctica
0°
90°W
90°E
180°
60°S
70°S
80°S
b
65°W
55°W
65°S
70°S
Antarctic Peninsula
Weddell Sea
c
Ulu P.
Vega Is.
Erebus and Terror Gulf
CWM
James Ross Island
Seymour Is.
Röhss Bay
Snowhill Is.
10 km
d
Herbert Sound
Ríos Point
Croft Bay
Clearwater Mesa
Soledad
Joanna
Martina
Graciela
Adela
Maria
Susan
Norma
Ileana
Linda
Karina
Joaquina
Silvia
Katerina
Ludmila
Esther
Alejandra
Adru
Natasha
Field camp 2015-2016
Valentina
Marta
Claudina
Sara
Sandra
Tatana
Paula
Nora
Tamara
Trinidad
Juanita
Adriana
Andrea
Argentina
Stark Point
Florencia
Blancmange Glacier
Cecilia
Haddington Ice Cap
N
64°1'S
64°1'30"S
64°2'S
64°2'30"S
0
1 km
Lake systems
Katerina
Trinidad-Tatana
Norma
Florencia
Isolated lakes
Sediment sample
Snowbank
Stream
Cliff headwall
57°45'W
57°44'W
57°43'W
57°42'W
57°41'W
57°40'W
57°39'W

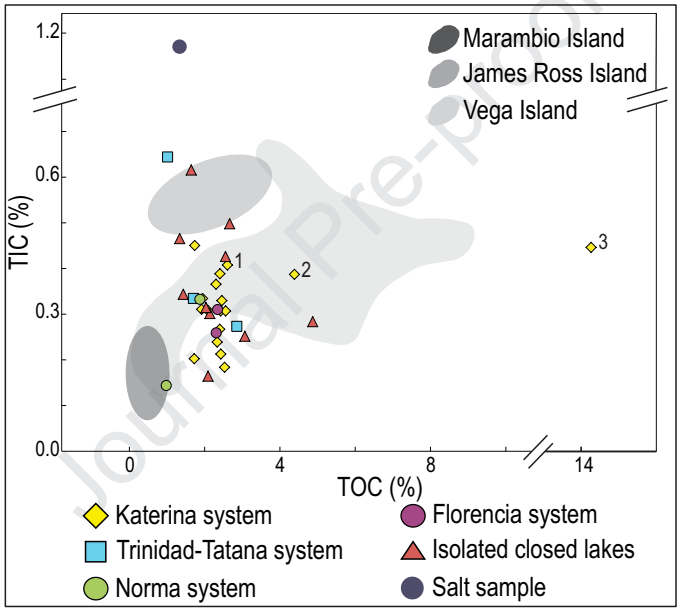

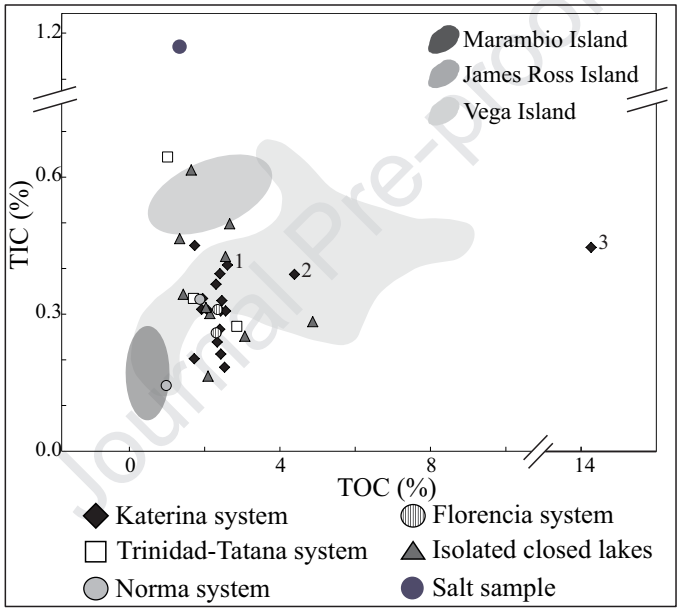

Bimodal	Trimodal silt	Trimodal sand
Adriana	Joaquina	Andrea
Adru	Katerina-2	Cecilia
Alejandra	Paula	Esther
Claudina	Sara	Graciela
Florencia	Susan	Juana
Ileana	Tamara	Katerina-3
Juanita		Linda
Karina		Ludmila
Katerina-1		Natasha
Maria		Norma
Marta		Silvia
Martina		Valentina
Nora		Salt
Soledad		
Tatana		
Trinidad		

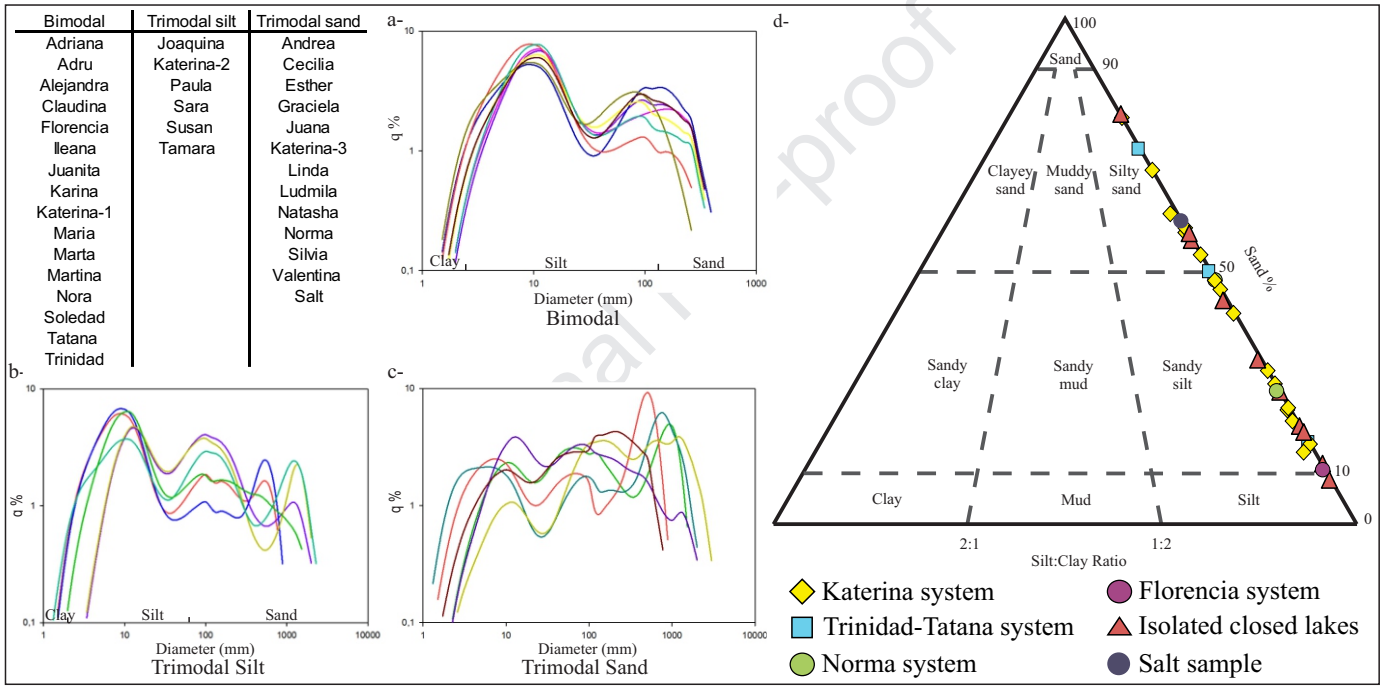

Bimodal	Trimodal silt	Trimodal sand
Adriana	Joaquina	Andrea
Adru	Katerina-2	Cecilia
Alejandra	Paula	Esther
Claudina	Sara	Graciela
Florencia	Susan	Juana
Ileana	Tamara	Katerina-3
Juanita		Linda
Karina		Ludmila
Katerina-1		Natasha
Maria		Norma
Marta		Silvia
Martina		Valentina
Nora		Salt
Soledad		
Tatana		
Trinidad		

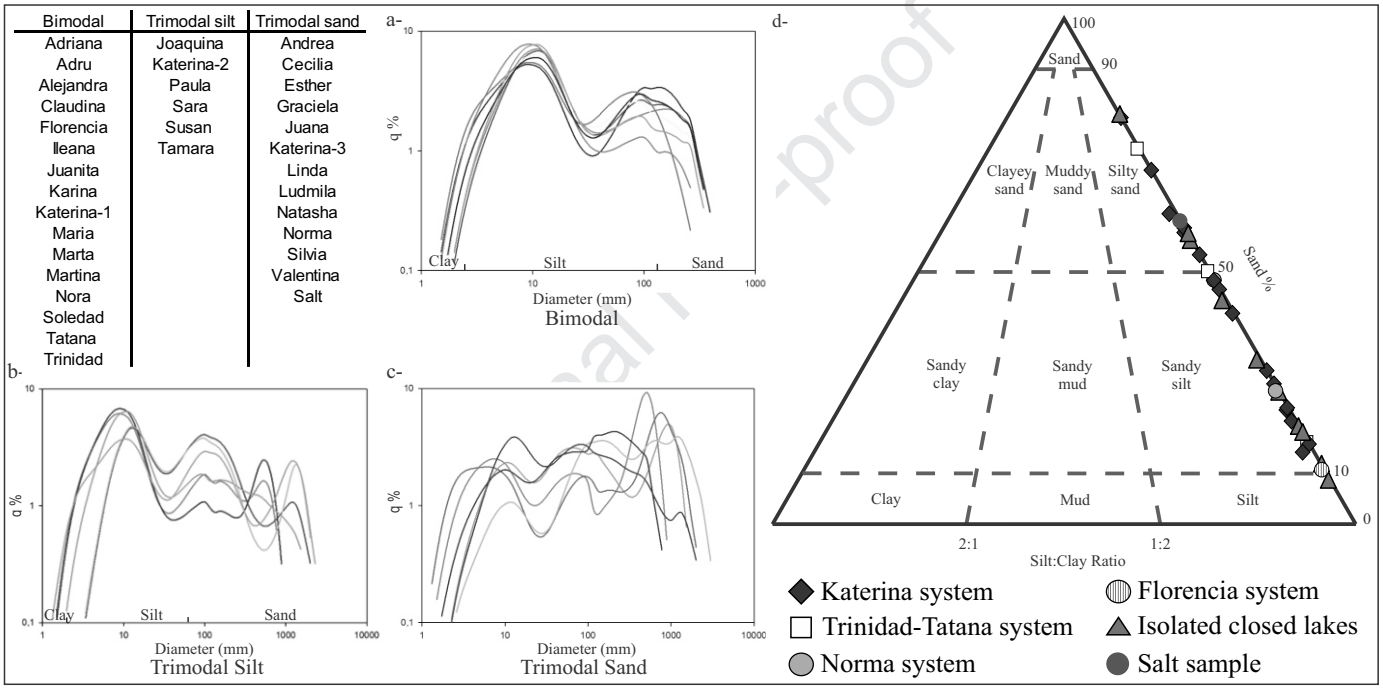

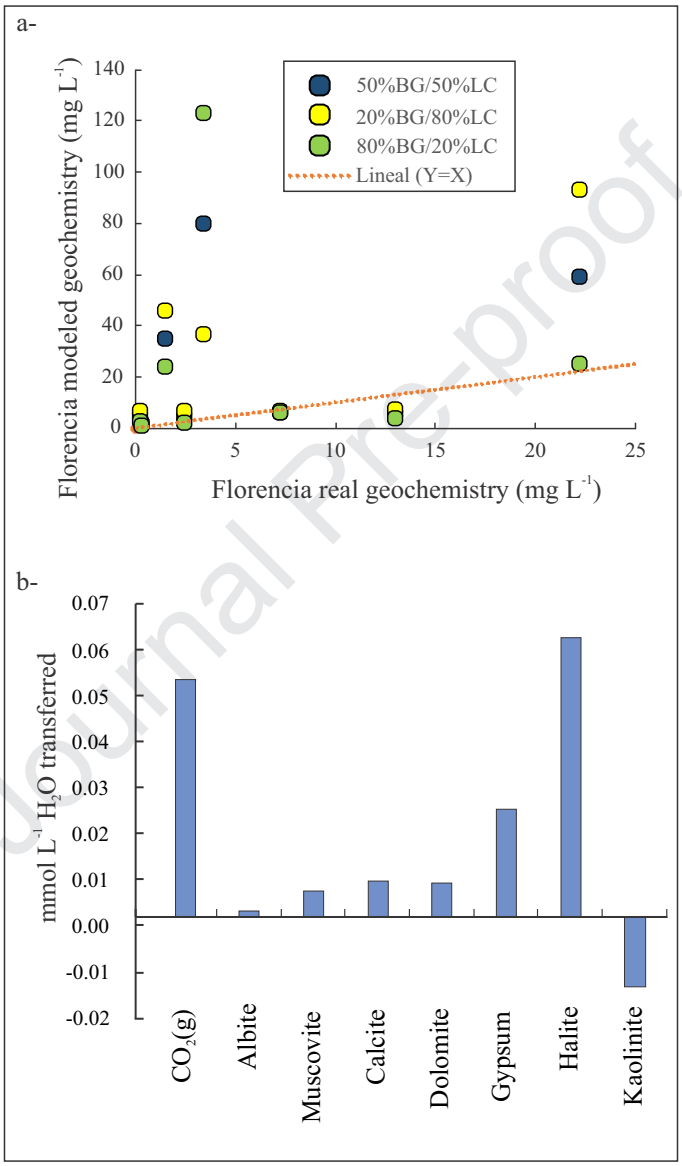

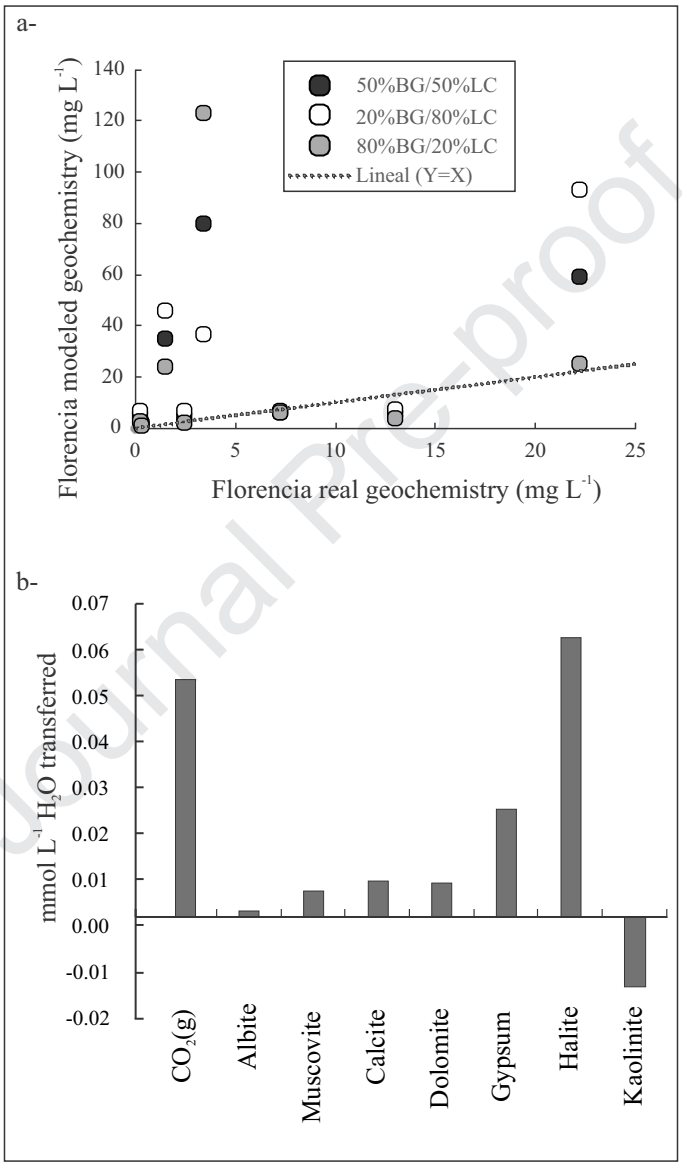

-Energy dissipates from external to internal lakes within drainage systems.

-Weathering influences lake chemistry along with sea spray, dilution, and evaporation.

-Minor/trace metals controlled by water-sediment and water-bedrock interactions.